2024
11(3), 668

Chemical Biology
LETTERS

Synthesis of new Nilutamide-pyrazole derivatives as VEGFR-2 targeting anti-prostate cancer agents

K. Swapna[1,2], Satheesh Kumar Nukala[1], N. Malla Reddy[3], Ravinder Manchal[1*]

[1]*Department of Chemistry, Chaitanya (Deemed to be University), Himayath Nagar, Moinabad, Ranga Reddy, Hyderabad, Telangana, India.* [2]*Department of Chemistry, R.B.V.R.R Womens College, Narayanaguda, Hyderabad, Telangana, India.* [3]*Department of Chemistry, Satavahana University, Karimnagar, Telangana, India.*

Submitted on: 26-Jan-2024, Accepted and Published on: 30-Apr-2024

Article

ABSTRACT

Herein, we synthesized new Nilutamide-pyrazoles (**6a-6n**) *via* N-alkynylation and $PdCl_2(PPh_3)_2$/CuI catalyzed tandem one-pot acyl-Sonogashira coupling followed by cyclo-condensation approaches. The *in vitro* anti-proliferative activity of these compounds against two human prostate cancer cell lines (PC-3 and DU-145) revealed that many of investigated compounds have shown better activity against PC-3 cell line as compared to DU-145 cell line. In particular, compounds **6d**, **6f** and **6m** had higher activity against PC-3 than the standard drug 5-Fluoro Uracil (5-FU) with IC_{50} values <65 μM. As well, compound **6f** displayed (IC_{50} = 39.1 μM) almost similar activity as 5-FU against DU-145 (IC_{50} = 38.5 μM). The *in vitro* VEGFR-2 inhibition studies revealed that compound **6f** showed higher activity (IC_{50} = 26.1 nM) against VEGFR-2 than the standard drug Sorafenib (IC_{50} = 30 nM), whereas, compound **6d** was shown comparable inhibition (IC_{50} = 30.6 nM) with the positive control. Finally, *in silico* molecular docking studies were described important binding interactions of most potent compounds **6d**, **6f**, **6m** and Sorafenib with VEGFR-2 (pdb id 3VHE) and these compounds showed promising binding energies and inhibition constants than the Sorafenib.

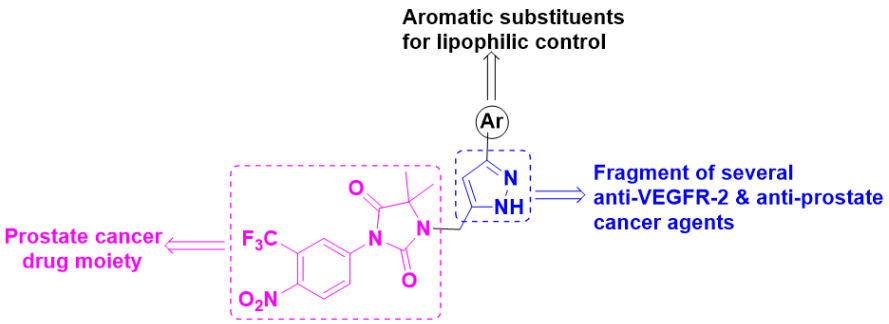

New Nilutamide-pyrazoles (6a-6n)
Anti-Prostate cancer and Anti-VEGFR-2 activity

Keywords: Nilutamide, pyrazole, anti-prostate cancer activity, VEGFR-2 inhibition

INTRODUCTION

In the majority of developed nations, prostate cancer is one of the most frequently diagnosed cancers and a major contributor to cancer-related death.[1] The invasiveness and metastasis of advanced prostate cancer are primarily responsible for the high death rate.[2] Therefore, one promising treatment approach for prostate cancer may involve focusing on the molecules responsible for metastasis. The Vascular endothelial growth factor (VEGFR-2) controls the signaling pathway that regulates the vascular permeability, survival, and migration of cancer cells.[3,4] It has been demonstrated that VEGF and its kinase receptors influence angiogenesis and the ability of newly formed blood vessels within tumor cells to survive.[5-7] Targeting this signaling pathway has the benefit that VEGF induction in tumor cells may arise from cancer-related alterations; VEGFR-2 expression is weak in healthy tissue and cells but is overexpressed in a number of cancer types, including prostate cancer.[8] Currently, one of the difficult tasks is to find new scaffolds that have ability to inhibit tyrosine kinase.[9-12] Hence, few FDA-approved anti-VEGFR agents (Sunitinib, Sorafenib, Venetanib, Axitinib, and Regorafenib) are available in the market. However, a significant downside with the monotherapy of these agents is drug resistance.[13-14]

One of the active non-steroidal antiandrogen (NSAA) drugs used to treat prostate cancer was Nilutamide. It functions as a selective antagonist of the androgen receptor by inhibiting the effects of testosterone and dihydrotestosterone on the body.[15-16] Because many prostate cancer cells rely on these hormones for growth and survival, Nilutamide could stop the prostate cancer

*Corresponding Author: Prof. Ravinder Manchal, Department of chemistry, Chaitanya (Deemed to be University), Himayath Nagar (V), Moinabad (M), Ranga Reddy (D), Hyderabad, Telangana, India

Email: visitravi76@gmail.com

URN:NBN:sciencein.cbl.2024.v11.668

https://pubs.thesciencein.org/cbl

from spreading and extend the lives of those who already have the condition.[15] However, due to few side effects of Nilutamide, other NSAAs which includes Bicalutamide and Enzalutamide have often replaced it.[16–20] Literature survey revealed that introducing amid,. predominantly, the incorporation of various pharmacophores such as aromatic amides, 1,2,3-triazoles[21] and isoxazoles on the cyclic amide ring of Nilitamide drug has been reported as potent anticancer agents against few human cancer cell lines.[22-24]

It is interesting to note that the pyrazole-tethered heterocycle compounds are a noteworthy class of compounds used in the cancer treatment.[25–32] Pyrazole compounds I and II (Figure. 1) were demonstrated to be effective anti-prostate cancer agents, similar to Sorafenib. Additionally, drugs based on heterocycles with substituted pyrazole ring have frequently been among the top-selling pharmaceutical products. For example, anticancer drugs Crizotinib and Ruxolitinib, which represent pyrazole-tethered anticancer drugs presently available in market.[33] The antitumor activity of Celecoxib was demonstrated by stimulating the formation of tumor micro-vessels and VEGF expression. Moreover, several reports highlight the antiproliferative effects of celecoxib against prostate tumors in experimental models.[34-36] Moreover, it has been reported that these pyrazole compounds, of which Pazopanib III, which is FDA-approved, and TAK-593 IV, which is undergoing phase one clinical investigation have excellent VEGFR-2 inhibition ability in addition to their antiproliferative potential. (**Figure 1**).[37–44]

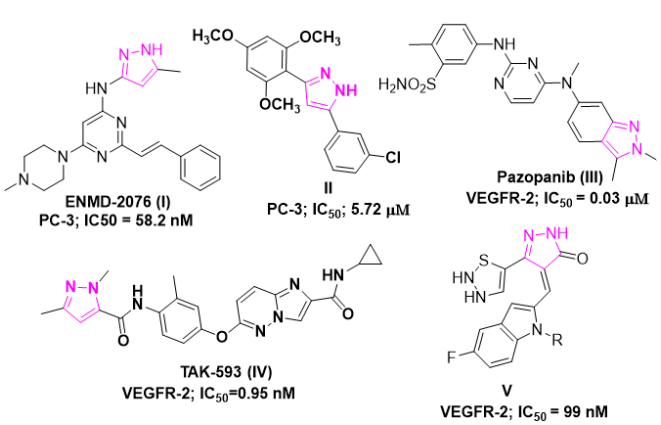

Figure 1. Few pyrazole containing antiproliferative or anti-VEGFR-2 compounds.

Given all the above considerations, in the present work, we report synthesis of new Nilutamide-pyrazole derivatives as VEGFR-2 targeting anti-prostate cancer agents (**Figure 2**).

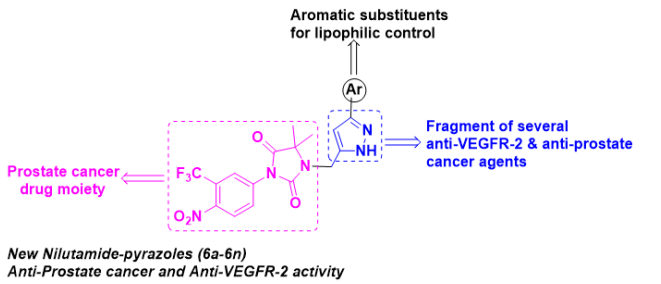

Figure 2. Designed strategy of Nilutamide-pyrazoles

RESULTS AND DISCUSSION

Chemistry

The synthesis of targeted Nilutamide-pyrazoles (**6a-6n**) was achieved in two main steps. First step involves the synthesis of key alkyne intermediate 5,5-dimethyl-3-(4-nitro-3-(trifluoromethyl)phenyl)-1-(prop-2-yn-1-yl)imidazolidine-2,4-dione (**3**) from the reaction between Nilutamide (5,5-dimethyl-3-(4-nitro-3-(trifluoromethyl)phenyl)imidazolidine-2,4-dione) (**1**) and 3-bromoprop-1-yne (**2**) in the presence of Cs_2CO_3 in MeCN at 80 °C for 7 h (**3**).

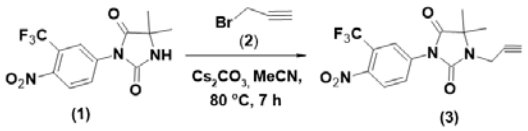

Scheme 1. Synthesis of 5,5-dimethyl-3-(4-nitro-3-(trifluoromethyl) phenyl)-1-(prop-2-yn-1-yl)imidazolidine-2,4-dione (**3**)

In the second step, we synthesized our desired compounds (**6a-6n**) using previously developed $PdCl_2(PPh_3)_2$/CuI catalyzed acyl Sonogashira coupling[45] and cyclocondesation strategies.[46] In detail, the $PdCl_2(PPh_3)_2$/CuI catalyzed acyl-Sonogashira coupling of alkyne intermediate **3** and aromatic acid chlorides (**4a-4n**) using K_2CO_3 and sodium lauryl sulfate in water at 65 °C after 7 h gave the corresponding *in situ* α,β-unsaturated ynones,[45] which were then treated with $N_2H_4.H_2O$ (**5**) for an additional 12 h to afford anticipated compounds (**6a-6n**).[46]

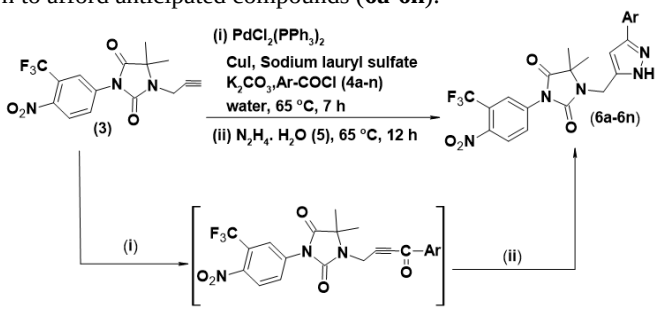

Scheme 2. Synthesis of Nilutamide-pyrazoles (**6a-6n**)

In vitro anti-prostate cancer activity

The newly synthesized Nilutamide-pyrazoles (**6a-6n**) were then evaluated for their *in vitro* anti-proliferative efficacy against two human prostate cancer cell lines (PC-3 and DU-145) with the help of MTT assay and here chemotherapeutic drug 5-FU was used as standard. According to Table 1, many of the evaluated compounds showed higher potency against PC-3 in comparison to the DU-145. In particular, compounds **6d** (IC_{50} = 61.1 µM), **6f** (IC_{50} = 41.7 µM) and **6m** (IC_{50} = 64.8 µM) displayed higher potency against PC-3 than the 5-FU (IC_{50} = 68.6 µM). In addition, compound **6f** (IC_{50} = 39.1 µM) had comparable inhibition against DU-145 with the positive control (IC_{50} = 38.5 µM). Furthermore, compounds **6c** and **6i** have shown promising activity against PC-3 in comparison to 5-FU with IC_{50} values = 70.2 and 71.1 µM respectively. However, the remaining

compounds showed good to poor activity on selected cell lines when compared with positive control.

The nature of aromatic substituents that attached to 3rd position of the pyrazole ring affecting anti-prostate cancer activity was also studied using structure-activity relationship (SAR) studies. At first, concerning electron-donating groups on the phenyl ring, compound **6f** with a 3-methoxy group showed better activity. Also compound **6d** containing the 3,5-diMe group was ranked second in this series. When we introduced a methoxy group 4th position (compound **6e**) and two methoxy substituents at 3rd and 5th positions (compound **6g**) led to decreased activity in comparison to compound **6f**. However, introducing methyl substitutions at 4th and 3rd position led to compounds **6b** and **6c** respectively showing poor activity than compound **6d**. Nonetheless, simple phenyl ring compound **6a** has shown reduced activity than all electron-releasing group-containing compounds.

In the case of electron-withdrawing groups on phenyl rings, compound **6m** containing 4-$COCH_3$ substituent showed better activity. The next better activity was shown by compound **6i** containing 4-Cl substituent. Compounds **6k** and **6l** bearing 4-NO_2 and 4-CN respectively, have shown weaker activity than the compound **6i.** However, compounds **6h** and **6j** bearing other halogen groups such as 4-F and 4-Br respectively have shown weaker activity than all the remaining compounds in this category.

Replacing the simple phenyl ring by a 4-pyridyl ring on pyrazole moiety led to compound **6n** showing slightly better activity than the compound **6a**.

Overall activity for the five most potent compounds against PC-3 was found as **6f>6d>6m>6c>6i.**

In vitro VEGFR-2 activity

The compounds **6c**, **6d, 6f, 6i** and **6m** which were more active against PC-3 were then screened for their *in vitro* VEGFR-2 inhibition potency and results were compared with the standard drug Sorafenib. Predominantly, compound **6f** showed remarkable activity (IC_{50} = 26.1 nM) against VEGFR-2 which was higher than the Sorafenib (IC_{50} = 30 nM). As well, compound **6d** displayed comparable activity (IC_{50} = 30.6 nM) to the positive control. Further, compounds **6m** showed the most promising activity as compared to positive control. However, compounds **6c** and **6i** have shown poor activity in comparison to the standard drug.

Table 1: *In vitro* anti-prostate cancer activity of compounds (**6a-6n**) with IC_{50} in µM[a]

Compound	Ar	[b]PC-3	[c]DU-145
6a	C_6H_5	90.6	NI
6b	4-MeC_6H_4	87.3	53.3
6c	3-MeC_6H_3	**70.2**	56.7
6d	3,5-diMeC_6H_3	**61.1**	**41.4**
6e	4-$OMeC_6H_4$	86.1	54.8
6f	3-$OMeC_6H_3$	**41.7**	**39.1**
6g	3,5-di$OMeC_6H_3$	80.3	48.2
6h	4-FC_6H_4	86.4	**63.5**
6i	4-ClC_6H_4	**71.1**	**51.7**
6j	4-BrC_6H_4	85.7	NI
6k	4-$NO_2C_6H_4$	84.1	56.8
6l	4-CNC_6H_4	79.8	60.2
6m	4-$COCH_3C_6H_4$	**64.8**	**40.2**
6n	4-pyridyl	86.2	61.3
5-FU		68.6	38.5

[a]All IC_{50} values are calculated as the mean of at least three different experiments.
[b]PC-3: Human prostate cancer cell line.
[c]DU-145: Human prostate cancer cell line.
NI = No inhibition (IC_{50} = >100 µM).

Table 2. VEGFR-2 inhibitory activity of compounds **6c**, **6d, 6f, 6i** and **6m**

Compound	IC $_{50}$ (nM)
6c	45.3
6d	**30.6**
6f	**26.1**
6i	48.1
6m	**33.6**
Sorafenib	30

*All IC_{50} values are calculated as the mean of at least three different experiments.

Table 3. Molecular docking interaction parameters of compounds (**6d, 6f** and **6m**) with the VEGFR-2 (pdb id 3VHE).

Entry	Binding Energy (kcal/mol)	Inhibition Constant	No. of hydrogen bonds	Residues involved in hydrogen bonding (bond length in Å)	Residues involved in Π–Π–stacking and Π–cation formation
6d	-9.91	54.16 nM	2	LYS868 (1.73), ASP1046 (1.94)	PHE1047
6f	-9.37	85.10 nM	-	-	-
6m	-9.52	65.37 nM	1	LYS868 (2.54)	PHE1047
Sorafenib	-8.96	95.9 nM	4	GLU885 (1.99), CYS919 (1.85, 2.28), ASP1046(1.76)	-

Molecular docking studies

Finally, we studied the *in silico* molecular docking studies of three potent compounds **6d**, **6f**, **6m** and the standard drug Sorafenib with VEGFR-2 (pdb id 3VHE) using Auto dock tools and this protein structure was downloaded from protein data bank.[47] The results revealed that compounds **6d**, **6f**, and **6m** displayed better binding energies (-9.37 to -9.91 kcal/mol) and inhibition constants (54.16 to 85.10 nM) than the standard drug Sorafenib (Binding energy = -8.96 kcal/mol) and 95.9 nM inhibition constant). Among them, compound **6d** exhibited greater binding energy (-9.91 kcal/mol) and 54.16 nM inhibition

constant. Compound **6m** was ranked second in this series with binding energy (-9.52 kcal/mol) and 65.37 nM inhibition constant. However, Compound **6f** exhibited least binding energy (-9.37 kcal/mol) and 85.10 nM inhibition constant. With respect to binding interactions, compound **6d** formed H-bond with LYS868 and ASP1046. Compound **6m** formed hydrogen bond with LYS868. Both compounds **6d** and **6m** formed π–π-stacking interaction with PHE1047. However, compound **6f** did not form any interaction with the residues of VEGFR-2. Predominantly, the standard drug Sorafenib formed hydrogen bonds with GLU885, CYS919 (two H-bonds) and ASP1046.

EXPERIMENTAL

General information

All the chemicals were purchased from different suppliers and used without any further purification. The purity of all compounds was assessed using Merck 60F254 silica gel plates. The ^{1}H & ^{13}C NMR spectra recorded with a Mercuryplus spectrometer (operating at 400 MHz for ^{1}H & 100 MHz for ^{13}C) chemical shifts were referenced to TMS. The ESI (electrospray ionization) mass spectra (ionizing voltage of 70 eV) were obtained using Shimadzu QP5050A quadrupole mass spectrometer. The CHN analysis was achieved with an Elemental Analyser Perkin–Elmer 240 C apparatus.

Synthesis of 5,5-dimethyl-3-(4-nitro-3-(trifluoromethyl)phenyl)-1-(prop-2-yn-1-yl)imidazolidine-2,4-dione (3): A mixture of 5,5-dimethyl-3-(4-nitro-3-(trifluoromethyl)phenyl)imidazolidine-2,4-dione (**1**) (0.0126 mol), Cs_2CO_3 (0.019 mmol) and 3-bromoprop-1-yne (**2**) (0.17 mmol) in MeCN (35 mL) was stirred at 80 °C for 7 h. After completion of the reaction as analyzed by the TLC, the reaction mixture was cooled to RT and filtered. The obtained filtrate was extracted with ethyl acetate (2 X 40 mL) and the combined organic layer was reduced under a rotary vacuum. Finally, the crude product was subjected to 60-120 mesh size silica gel column chromatography using (3:7) ethyl acetate/hexane as eluent. 73% yield; Yellow solid; M.P.156-158 °C; ^{1}H NMR (400 MHz, $CDCl_3$): δ 8.09 (s, 1H), 8.01 (d, *J* = 7.7 Hz, 1H), 7.71 (d, *J* = 7.7 Hz, 1H), 4.08 (s, 2H), 2.27 (s, 1H), 1.44 (s, 6H) ppm.

Procedure for the synthesis of Nilutamide-pyrazole hybrids (6a-6n): A mixture of $PdCl_2(PPh_3)_2$ (0.01 mmol), CuI (0.03 mmol), sodium lauryl sulfate (0.05 mmol), benzoyl chloride **4a** (1.0 mmol), K_2CO_3 (1.5 mmol) and intermediate **3** (0.5 mmol) in 5 mL of water was stirred at 65 °C for 7 h. The formation of respective *in situ* ynone was analyzed by the TLC, then N_2H_4. H_2O (**5**) (1.0 mmol) was added and stirring was continued for an additional 12 h. Later, the reaction mixture was cooled and extracted with ethyl acetate (2 X 10 mL). The excess of the organic layer was concentrated under a vacuum. The resulting crude product was purified by 60-120 mesh size silica gel column chromatography using ethyl acetate/hexane (1:1) as eluent.

5,5-dimethyl-3-(4-nitro-3-(trifluoromethyl)phenyl)-1-((3-phenyl-1*H*-pyrazol-5-yl)methyl)imidazolidine-2,4-dione (**6a**): Colorless solid; Yield 74%; M.P. 191-193 °C; ^{1}H NMR (400 MHz, DMSO-d_6) δ 13.05 (br s, 1H) 8.15 (s, 1H), 8.05 (d, *J* = 7.7 Hz, 1H), 7.82-7.74 (m, 4H). 7.45-7.38 (m, 2H), 7.14 (s, 1H), 4.72 (s, 2H), 1.48 (s, 6H) ppm; ^{13}C NMR (100 MHz, DMSO-d_6) δ 175.3, 156.1, 150.1, 146.6, 144.3, 133.1, 132.3, 130.6, 129.7, 129.1, 128.5, 128.1, 127.3, 124.9, 124.2, 99.6, 60.2, 44.5, 24.8 ppm; MS (ESI): m/z = 474 $[M+H]^+$; CHN analysis for $C_{22}H_{18}F_3N_5O_4$; Cacld (%): C, 55.82; H, 3.83; N, 14.79; Found (%): C, 55.85; H, 3.81; N, 14.77.

5,5-dimethyl-3-(4-nitro-3-(trifluoromethyl)phenyl)-1-((3-(p-tolyl)-1*H*-pyrazol-5-yl)methyl)imidazolidine-2,4-dione **(6b)**: Colorless solid; Yield 74%; M.P. 194-196 °C; ^{1}H NMR (400 MHz, DMSO-d_6) δ 13.03 (br s, 1H) 8.16 (s, 1H), 8.06 (d, *J* = 7.7 Hz, 1H), 7.82 (d, *J* = 7.8 Hz, 2H), 7.75 (d, *J* = 7.7 Hz, 1H), 7.31 (d, *J* = 7.8 Hz, 2H), 7.13 (s, 1H), 4.71 (s, 2H), 2.41 (s, 3H), 1.49 (s, 6H) ppm; ^{13}C NMR (100 MHz, DMSO-d_6) δ 175.2, 156.1, 149.9, 146.5, 144.4, 138.2, 134.1, 132.2, 130.4, 129.7, 129.2, 128.4, 127.3, 124.5, 124.1, 99.4, 60.3, 44.2, 24.9, 22.1 ppm; MS (ESI): m/z = 488 $[M+H]^+$; CHN analysis for $C_{23}H_{20}F_3N_5O_4$; Calcd (%):C, 56.67; H, 4.14; N, 14.37; Found (%): C, 56.69; H, 4.17; N, 14.39.

5,5-dimethyl-3-(4-nitro-3-(trifluoromethyl)phenyl)-1-((3-(m-tolyl)-1H-pyrazol-5-yl)methyl)imidazolidine-2,4-dione **(6c):** Cream solid; Yield 72%; M.P. 195-197 °C; ^{1}H NMR (400 MHz, DMSO-d_6) δ 13.07 (br s, 1H) 8.15 (s, 1H), 8.06 (d, *J* = 7.7 Hz, 1H), 7.74 (d, *J* = 7.7 Hz, 1H), 7.57-7.51 (m, 2H), 7.39 (t, J = 7.6 Hz, 1H), 7.31-7.24 (m, 1H), 7.14 (s, 1H), 4.73 (s, 2H), 2.38 (s, 3H), 1.48 (s, 6H) ppm; ^{13}C NMR (100 MHz, DMSO-d_6) δ 175.2, 156.2, 150.8, 146.7, 144.3, 140.2, 134.3, 132.4, 130.6, 129.8, 129.3, 128.8, 128.3, 127.7, 124.8, 124.3, 123.3, 99.6, 60.2, 44.7, 24.7, 21.9 ppm; MS (ESI): m/z = 510 $[M+Na]^+$; CHN analysis for $C_{23}H_{20}F_3N_5O_4$; Cacld (%): C, 56.67; H, 4.14; N, 14.37; C, 56.70; H, 4.12; N, 14.38.

1-((3-(3,5-dimethylphenyl)-1*H*-pyrazol-5-yl)methyl)-5,5-dimethyl-3-(4-nitro-3-(trifluoromethyl)phenyl)imidazolidine-2,4-dione (**6d**): Grey solid; Yield 68%; M.P. 199-201 °C; ^{1}H NMR (400 MHz, DMSO-d_6) δ 13.05 (br s, 1H), 8.16 (s, 1H), 8.05 (d, *J* = 7.7 Hz, 1H), 7.74 (d, *J* = 7.7 Hz, 1H), 7.48 (s, 2H), 7.13 (s, 1H), 7.06 (s, 1H), 4.72 (s, 2H), 2.40 (s, 6H), 1.47 (s, 6H) ppm; ^{13}C NMR (100 MHz, DMSO-d_6) δ 175.3, 156.2, 151.1, 146.6, 144.4, 140.6, 134.8, 132.3, 130.5, 129.7, 129.1, 128.4, 126.4, 124.7, 124.1, 99.4, 60.3, 44.5, 24.7, 22.2 ppm; MS (ESI): m/z = 502 $[M+H]^+$.

1-((3-(4-methoxyphenyl)-1H-pyrazol-5-yl)methyl)-5,5-dimethyl-3-(4-nitro-3-(trifluoromethyl)phenyl)imidazolidine-2,4-dione (**6e**): Light Yellow solid; Yield 69%; M.P. 198-200 °C; ^{1}H NMR (400 MHz, DMSO-d_6) δ 13.02 (br s, 1H), 8.17 (s, 1H), 8.07 (d, *J* = 7.7 Hz, 1H), 7.75 (d, *J* = 7.7 Hz, 1H), 7.59 (d, *J* = 7.4 Hz, 2H), 7.11 (s, 1H), 6.95 (d, *J* = 7.4 Hz, 2H), 4.71 (s, 2H), 3.89 (s, 3H), 1.49 (s, 6H) ppm; ^{13}C NMR (100 MHz, DMSO-d_6) δ 175.5, 159.3, 156.1, 150.2, 146.7, 144.5, 132.2, 130.4, 129.9, 129.3, 128.4, 125.9, 124.8, 114.8, 124.4, 99.4, 60.3, 56.8, 44.4, 24.8 ppm; MS (ESI): m/z = 504 $[M+H]^+$.

1-((3-(3-methoxyphenyl)-1*H*-pyrazol-5-yl)methyl)-5,5-dimethyl-3-(4-nitro-3-(trifluoromethyl)phenyl)imidazolidine-2,4-dione **(6f):** Colorless solid; Yield 71%; M.P. 199-201 °C; ^{1}H NMR (400 MHz, DMSO-d_6) δ 13.06 (br s, 1H), 8.15 (s, 1H), 8.05

(d, *J* = 7.7 Hz, 1H), 7.75 (d, *J* = 7.7 Hz, 1H), 7.47 (t, J = 7.3 Hz, 1H), 7.29-7.23 (m, 2H), 7.12 (s, 1H), 6.94 (dd, J = 7.2 Hz, 1.6 Hz, 1H), 4.70 (s, 2H), 3.87 (s, 3H), 1.48 (s, 6H) ppm; ^{13}C NMR (100 MHz, DMSO-d_6) δ 175.2, 161.8, 156.2, 150.7, 146.6, 144.4, 135.3, 132.4, 130.5, 130.1, 129.7, 128.5, 124.8, 124.3, 119.3, 118.5, 114.1, 99.3, 60.4, 56.5, 44.3, 24.7 ppm; MS (ESI): m/z = 504 $[M+H]^+$; CHN analysis for $C_{23}H_{20}F_3N_5O_5$; Cacld (%): C, 54.87; H, 4.00; N, 13.91; Found (%): C, 54.90; H, 4.02; N, 13.94.

1-((3-(3,5-dimethoxyphenyl)-1*H*-pyrazol-5-yl)methyl)-5,5-dimethyl-3-(4-nitro-3-(trifluoromethyl)phenyl)imidazolidine-2,4-dione (**6g**): Light orange solid; Yield 66%; M.P. 206-208 ºC; ^{1}H NMR (400 MHz, DMSO-d_6) δ 13.04 (br s, 1H), 8.16 (s, 1H), 8.06 (d, *J* = 7.7 Hz, 1H), 7.74 (d, *J* = 7.7 Hz, 1H), 7.21 (s, 2H), 7.14 (s, 1H), 6.70 (s, 1H), 4.72 (s, 2H), 3.91 (s, 6H), 1.47 (s, 6H) ppm; ^{13}C NMR (100 MHz, DMSO-d_6) δ 175.4, 162.6, 156.3, 151.1, 146.5, 144.3, 137.1, 132.2, 130.6, 129.9, 128.6, 124.7, 124.1, 107.5, 100.6, 99.6, 60.3, 56.9, 44.6, 24.7 ppm; MS (ESI): m/z = 556 $[M+Na]^+$; CHN analysis for $C_{24}H_{22}F_3N_5O_6$; Cacld (%): C, 54.04; H, 4.16; N, 13.13; Found (%): C, 54.06; H, 4.18; N, 13.16;

1-((3-(4-fluorophenyl)-1*H*-pyrazol-5-yl)methyl)-5,5-dimethyl-3-(4-nitro-3-(trifluoromethyl)phenyl) imidazolidine-2,4-dione (**6h**): Colorless solid; Yield 79%; M.P. 193-195 ºC; ^{1}H NMR (400 MHz, DMSO-d_6) δ 13.12 (br s, 1H), 8.17 (s, 1H), 8.07 (d, *J* = 7.7 Hz, 1H), 7.76 (d, *J* = 7.7 Hz, 1H), 7.54 (d, *J* = 7.2 Hz, 2H), 7.20 (s, 1H), 7.12 (d, J = 7.3 Hz, 2H), 4.74 (s, 2H), 1.48 (s, 6H) ppm; ^{13}C NMR (100 MHz, DMSO-d_6) δ 175.5, 160.9, 156.2, 150.3, 146.7, 144.4, 132.5, 130.6, 130.2, 129.8, 129.1, 128.4, 124.8, 124.2, 116.6, 100.1, 60.2, 44.8, 24.8 ppm; MS (ESI): m/z = 492 $[M+H]^+$.

1-((3-(4-chlorophenyl)-1*H*-pyrazol-5-yl)methyl)-5,5-dimethyl-3-(4-nitro-3-(trifluoromethyl)phenyl) imidazolidine-2,4-dione (**6i**): Cream solid; Yield 78%; M.P. 196-198 ºC; ^{1}H NMR (400 MHz, DMSO-d_6) δ 13.09 (br s, 1H), 8.17 (s, 1H), 8.06 (d, *J* = 7.7 Hz, 1H), 7.73-7.78 (m, 3H), 7.36 (d, *J* = 7.7 Hz, 2H), 7.18 (s, 1H), 4.72 (s, 2H), 1.47 (s, 6H) ppm; ^{13}C NMR (100 MHz, DMSO-d_6) δ 175.3, 156.2, 150.3, 146.5, 144.2, 134.3, 133.8, 132.3, 130.5, 129.9, 129.5, 129.1, 128.6, 124.7, 124.1, 60.3, 99.8, 44.5, 24.7 ppm; MS (ESI): m/z = 508 $[M+H]^+$; CHN analysis for $C_{22}H_{17}ClF_3N_5O_4$; Cacld (%): C, 52.03; H, 3.37; N, 13.79; Found (%): C, 52.04; H, 3.39; N, 13.76.

1-((3-(4-bromophenyl)-1*H*-pyrazol-5-yl)methyl)-5,5-dimethyl-3-(4-nitro-3-(trifluoromethyl)phenyl) imidazolidine-2,4-dione **(6j):** Light orange solid; Yield 75%; M.P. 212-212 ºC; ^{1}H NMR (400 MHz, DMSO-d_6) δ 13.06 (br s, 1H), 8.15 (s, 1H), 8.05 (d, *J* = 7.7 Hz, 1H), 7.82-7.74 (m, 3H), 7.43 (d, *J* = 7.9 Hz, 2H), 7.15 (s, 1H), 4.73 (s, 2H), 1.48 (s, 6H) ppm; ^{13}C NMR (100 MHz, DMSO-d_6) δ 175.4, 156.3, 150.3, 146.6, 144.4, 133.1, 132.4, 131.1, 130.4, 129.8, 128.5, 128.1, 124.8, 124.3, 123.1, 99.6, 60.4, 44.7, 24.8 ppm; MS (ESI): m/z = 552 $[M+H]^+$; CHN analysis for $C_{22}H_{17}BrF_3N_5O_4$; Cacld (%): C, 47.84; H, 3.10; N, 12.68; Found (%): C, 47.86; H, 3.13; N, 12.65.

5,5-dimethyl-3-(4-nitro-3-(trifluoromethyl)phenyl)-1-((3-(4-nitrophenyl)-1*H*-pyrazol-5-yl)methyl)imidazolidine-2,4-dione **(6k):** Light yellow solid; Yield 62%; M.P. 207-209 ºC; δ 13.13 (br s, 1H), 8.21-8.16 (m, 3H), 8.08 (d, *J* = 7.7 Hz, 1H), 7.83 (d, *J* = 7.3 Hz, 2H), 7.76 (d, *J* = 7.7 Hz, 1H), 7.21 (s, 1H), 4.75 (s, 2H), 1.51 (s, 6H) ppm; ^{13}C NMR (100 MHz, DMSO-d_6) δ 175.5, 156.2, 150.3, 148.6, 146.8, 144.4, 136.6, 132.5, 130.7, 129.9, 128.6, 127.1, 125.8, 125.1, 124.3, 100.5, 60.4, 44.9, 25.1 ppm; MS (ESI): m/z = 541 $[M+Na]^+$; CHN analysis for $C_{22}H_{17}F_3N_6O_6$; Cacld (%): C, 50.97; H, 3.31; N, 16.21; Found (%): C, 50.95; H, 3.33; N, 16.24.

4-(5-((5,5-dimethyl-3-(4-nitro-3-(trifluoromethyl)phenyl)-2,4-dioxoimidazolidin-1-yl)methyl)-1*H*-pyrazol-3-yl)benzonitrile (**6l**): Light Orange solid; Yield 73%; M.P. 197-199 ºC; δ ^{1}H NMR (400 MHz, DMSO-d_6) 13.09 (br s, 1H), 8.16 (s, 1H), 8.07 (d, *J* = 7.7 Hz, 1H), 7.86 (d, *J* = 7.9 Hz, 2H), 7.75 (d, *J* = 7.7 Hz, 1H), 7.47 (d, *J* = 7.9 Hz, 2H), 7.17 (s, 1H), 4.73 (s, 2H), 1.47 (s, 6H) ppm; ^{13}C NMR (100 MHz, DMSO-d_6) δ 175.3, 156.3, 150.1, 146.7, 144.4, 138.1, 134.2, 132.4, 130.9, 130.5, 129.8, 128.5, 124.8, 124.2, 119.9, 115.3, 99.8, 60.2, 44.7, 24.7 ppm; MS (ESI): m/z = 499 $[M+H]^+$; CHN analysis for $C_{23}H_{17}F_3N_6O_4$; Cacld (%): C, 55.43; H, 3.44; N, 16.86; Found (%): C, 55.46; H, 3.45; N, 16.89.

1-((3-(4-acetylphenyl)-1*H*-pyrazol-5-yl)methyl)-5,5-dimethyl-3-(4-nitro-3-(trifluoromethyl)phenyl)imidazolidine-2,4-dione **(6m):** Colorless solid; Yield 76%; ^{1}H NMR (400 MHz, DMSO-d_6) δ 13.11 (br s, 1H), 8.17 (s, 1H), 8.06 (d, *J* = 7.7 Hz, 1H), 7.94 (d, *J* = 7.6 Hz, 2H), 7.75-7.68 (m, 3H), 7.18 (s, 1H), 4.73 (s, 2H), 2.59 (s, 3H), 1.48 (s, 6H) ppm; ^{13}C NMR (100 MHz, DMSO-d_6) δ 197.6, 175.5, 156.3, 150.3, 146.8, 144.3, 141.1, 135.6, 132.5, 130.6, 129.9, 128.9, 128.4, 124.9, 124.3, 99.9, 60.4, 44.8, 29.4, 24.9 ppm; MS (ESI): m/z = 516 $[M+H]^+$; CHN analysis for $C_{24}H_{20}F_3N_5O_5$; Cacld (%): C, 55.92; H, 3.91; N, 13.59; Found (%): C, 55.94; H, 3.87; N, 13.61.

5,5-dimethyl-3-(4-nitro-3-(trifluoromethyl)phenyl)-1-((3-(pyridin-4-yl)-1*H*-pyrazol-5-yl)methyl)imidazolidine-2,4-dione **(6n):** Light Brown solid; Yield 72%; M.P. 194-196 ºC; ^{1}H NMR (400 MHz, DMSO-d_6) δ 13.08 (br s, 1H), 8.78 (d, *J* = 7.8 Hz, 2H), 8.15 (s, 1H), 8.05 (d, *J* = 7.7 Hz, 1H), 7.76 (d, *J* = 7.7 Hz, 1H), 7.61 (d, *J* = 7.8 Hz, 2H), 7.13 (s, 1H), 4.71 (s, 2H), 1.47 (s, 6H) ppm; ^{13}C NMR (100 MHz, DMSO-d_6) δ 175.3, 156.2, 152.7, 150.1, 146.7, 144.3, 136.1, 132.4, 130.4, 129.8, 128.5, 124.8, 124.2, 120.5, 99.5, 60.2, 44.5, 24.8 ppm; MS (ESI): m/z = 475 $[M+H]^+$; CHN analysis for $C_{21}H_{17}F_3N_6O_4$; Cacld (%): C, 53.17; H, 3.61; N, 17.72; Found (%): C, 53.18; H, 3.64; N, 17.70.

MTT assay

96-well tissue culture microtiter plates were used and every well received 100 µL of complete media comprising 1×10^4 cells as an inoculum. Preceding to experiment, the plates were incubated at 37 ºC in a humidified 5% CO_2 incubator for 18 h. After removing the medium, each well received 100 µL of fresh medium containing the test compounds and 5-FU at concentrations 0.5, 1 and 2 µM. This medium was incubated at 37 ºC for 24 h. The medium was then discarded, and 10 µL of MTT dye was added in its place. For 2 h, plates were incubated

at 37 ºC. In 100 µL of extraction buffer, the resultant formazan crystals were solubilized. Using a microplate reader, the optical density (O.D.) was read at 570 nm (Multi-mode Varioskan Instrument-Themo Scientific). Never did the medium contain more DMSO than 0.25%.

VEGFR-2 enzyme activity

Compounds **6c**, **6d**, **6f**, **6i** and **6m** were screened for their capability to inhibit VEGFR-2 kinase activity using a VEGFR2 (KDR) kinase assay kit (BPS Bioscience, Corporation catalog # 40325) according to the manufacturer's protocol.

CONCLUSION

In summary, we extended the application of previously developed $PdCl_2(PPh_3)_2$/CuI catalyzed acyl-Sonogashira coupling[45] and cyclo-condensation[46] approaches to synthesize some new Nilutamide containing pyrazoles (**6a-6n**) in eco-friendly water solvent without isolation of any α,β-unsaturated ynones. The preliminary anti-prostate cancer activity studies revealed that compounds **6d**, **6f** and **6m** were more active over PC-3 cell lines than the standard drug 5-FU. In specific, the compound **6f** (IC_{50} = 41.7 µM) was found to be >1.5 times potent than the 5-FU (IC_{50} = 68.6 µM) against PC-3 cell line. The potent compounds (**6c**, **6d, 6f, 6i** and **6m)** found against PC3 cell lines were then screened for their *in vitro* anti-VEGFR-2 efficacy and found that compound **6f** had greater activity than the standard drug Sorafenib with IC_{50} value 26.1 nM, while, compound **6d** (IC_{50} = 30.6 nM) showed almost similar potency with the Sorafenib (IC_{50} = 30 nM). Finally, molecular docking studies revealed that the compounds **6d**, **6f** and **6m** showed better binding energies and inhibition constants on VEGFR-2 (pdb id 3VHE) than the Sorafenib. Further anticancer mechanism studies are under progress.

SUPPLEMENTARY INFORMATION

The molecular docking and NMR data images are provided as supplementary file which can be downloaded from article page/journal site.

ACKNOWLEDGMENTS

Authors are thankful to Chaitanya (Deemed to be University), Hyderabad campus, for providing research facilities. The author K. Swapna is thankful to R.B.V.R.R Womens College, Narayanaguda, Hyderabad for constant support during this work.

CONFLICT OF INTEREST STATEMENT

Authors do not have any financial or academic or otherwise conflict of interest for this work.

REFERENCES

1. B.S. Chhikara, K. Parang. Global Cancer Statistics 2022: the trends projection analysis. *Chem. Biol. Lett.* **2023**, 10 (1), 451.
2. D.P. Petrylak, Future directions in the treatment of androgen-independent prostate cancer. *Urology*. **2005**, 65, 8–12.
3. G. McMahon, VEGF Receptor Signaling in Tumor Angiogenesis. *Oncologist*. **2000**, 5, 3-10.
4. D. Shweiki, A. Itin, D. Soffer, E. Keshet, Vascular endothelial growth factor induced by hypoxia may mediate hypoxia-initiated angiogenesis. *Nature*. **1992**, 359, 843-845.
5. A.K. Olsson, A. Dimberg, J. Kreuger, L. C. Welsh, VEGF receptor signalling? In control of vascular function. *Nat. Rev. Mol. Cell Biol*. **2006**, 7, 359-371.
6. R.S. Apte, D.S. Chen, N. Ferrara, VEGF in Signaling and Disease: Beyond Discovery and Development. *Cell*. **2019**, 176, 1248-1264.
7. M. Shibuya, Vascular endothelial growth factor and its receptor system: physiological functions in angiogenesis and pathological roles in various diseases. *J. Biochem*. **2013**, 153, 13-19.
8. S.J. Modi, V.M. Kulkarni, Vascular Endothelial Growth Factor Receptor (VEGFR-2)/KDR Inhibitors: Medicinal Chemistry Perspective. *Med. Drug Discovery*. **2019**, 2, 100009.
9. M. Fischer, Approved and Experimental Small-Molecule Oncology Kinase Inhibitor Drugs: A Mid-2016 Overview, *Med. Res. Rev*. **2017**, 37, 314-367.
10. N. Berndt, R.M. Karim, E. Schonbrunn, Advances of small molecule targeting of kinases, *Curr. Opin. Chem. Biol*. **2017**, 39, 126-132.
11. D. Fabbro, 25 Years of Small Molecular Weight Kinase Inhibitors: Potentials and Limitations, *Mol. Pharmacol*. **2015**, 87, 766-775.
12. M.E. Breen, M.B. Soellner, Small Molecule Substrate Phosphorylation Site Inhibitors of Protein Kinases: Approaches and Challenges, *ACS Chem. Biol*. **2015**, 10, 175-189.
13. G. Bergers, D. Hanahan, Modes of resistance to anti-angiogenic therapy, *Nat. Rev. Cancer*. **2008**, 8, 592-603.
14. R.N. Gacche, R.J. Meshram, Angiogenic factors as potential drug target: Efficacy and limitations of anti-angiogenic therapy. *Biochim. Biophys. Acta, Rev. Cancer*. **2014**, 1846, 161-179.
15. R.Z. Szmulewitz, E.M. Posadas. Antiandrogen therapy in prostate cancer. *Update Cancer Ther*. **2007**, 2 (3), 119–131.
16. E.J. Dole, M.T. Holdsworth, Nilutamide: an antiandrogen for the treatment of prostate cancer. *Ann Pharmacother*. **1997**, 31, 65-75.
17. I.D. Cockshott. Bicalutamide: Clinical pharmacokinetics and metabolism. *Clin. Pharmacokinet.* **2004**, 43 (13), 855–878.
18. J. Hoffman-Censits, W.K. Kelly. Enzalutamide: A novel antiandrogen for patients with castrate-resistant prostate cancer. *Clin. Cancer Res.* **2013**, 19 (6), 1335–1339.
19. L. Wang, M. Xu, C.-Y. Kao, S. Y. Tsai, M.J. Tsai, Small molecule JQ1 promotes prostate cancer invasion via BET-independent inactivation of FOXA1. *J. Clin. Invest.* **2020**, 130, 1782–1792.
20. R. Dhingra, T. Sharma, S. Singh, et al. Enzalutamide: A Novel Anti-androgen with Prolonged Survival Rate in CRPC Patients. *Mini-Reviews Med. Chem.* **2013**, 13 (10), 1475–1486.
21. P. Chaya, A.A. Cheriyan, S. Shah, et al. Synthesis and medicinal applications of quinoline hybrid heterocycles: a comprehensive review. *J. Mol. Chem.* **2022**, 2 (1), 338.
22. T. Narasimha Swamy, N. Satheesh Kumar, S. Narsimha, M. Ravinder, G. Prasad, P. Suresh, Design and Synthesis of Some Novel Aromatic Amide Derivatives of Nilutamide as In Vitro Anticancer Agents, *ChemistrySelect*. **2020**, 5, 12317-12319.
23. N. Malla Reddy, V. Rajender, A. Jeyanthi, Design and synthesis of new Nilutamide-1,2,3-triazole derivatives as in vitro Anticancer agents. *Chem. Biol. Lett*. **2022**, 9, 405.
24. A. Nagaraju, S. K. Nukala, T. N. Swamy, R. Manchal, Anti-prostate cancer and anti-EGFR activities of new Nilutamide-isoxazole hybrids. *Chem. Biol. Lett*. **2023**, 10, 542.
25. Koca, A. Ozgur, K.A. Coşkun, Y. Tutar, Synthesis and anticancer activity of acyl thioureas bearing pyrazole moiety. *Bioorg. Med. Chem*. **2013**, 21, 3859-3865.
26. M. Dawood, T.M.A. Eldebss, H.S.A.E. Zahabi, M. H. Yousef, P. Metz, Synthesis of some new pyrazole-based 1,3-thiazoles and 1,3,4-thiadiazoles as anticancer agents. *Eur. J. Med. Chem*. **2013**, 70, 740-749.
27. R.A. Abdellatif, E. K. A. Abdelall, M.A. Abdelgawad, R.R. Ahmed, R.B. Bakr, Synthesis and Anticancer Activity of Some New Pyrazolo[3,4-d]pyrimidin-4-one Derivatives. *Molecules*. **2014**, 19, 3297-3309.
28. C.H. Tu, W.H. Lin, Y.H. Peng et.al., Pyrazolylamine Derivatives Reveal the Conformational Switching between Type I and Type II Binding Modes of Anaplastic Lymphoma Kinase (ALK). *J. Med. Chem*. **2016**, 59, 3906-3919.

29. F.E. Bennani, L. Doudach, Y. Cherrah, Y. Ramli, K. Karrouchi, M. Ansar, M.E.A. Faouzi, Overview of recent developments of pyrazole derivatives as an anticancer agent in different cell line. *Bioorg. Chem*. **2020**, 97, 103470.
30. D. Havrylyuk, B. Zimenkovsky, O. Vasylenko, A. Gzella, R. Lesyk, Synthesis of New 4-Thiazolidinone-, Pyrazoline-, and Isatin-Based Conjugates with Promising Antitumor Activity. *J. Med. Chem*. **2012**, 55, 8630-8641.
31. H.H. Fahmy, N.M. Khalifa, M.M.F. Ismail, H.M. El-Sahrawy, E.S. Nossier, Biological Validation of Novel Polysubstituted Pyrazole Candidates with in Vitro Anticancer Activities. *Molecules*. **2016**, 21, 271.
32. G.M. Nitulescu, C. Draghici, O.T. Olaru, New Potential Antitumor Pyrazole Derivatives: Synthesis and Cytotoxic Evaluation. *Int. J. Mol. Sci*. **2013**, 14, 21805-21818.
33. J. Monga, N.S. Ghosh, S. Kamboj, M. Mukhija. Pyrazole derivatives affinity to Estrogen receptor Alpha for breast cancer treatment evaluation using molecular docking. *J. Mol. Chem.* **2023**, 3 (2), 590.
34. A.L. Hsu, T. T. Ching, D. S. Wang, X. Song, V. M. Rangnekar, C. S. Chen, The cyclooxygenase-2 inhibitor celecoxib induces apoptosis by blocking Akt activation in human prostate cancer cells independently of Bcl-2. *J. Biol. Chem*. **2000**, 275, 11397-11403.
35. S.K. Kulp, Y.T. Yang, C.C. Hung et.al. 3-Phosphoinositide-Dependent Protein Kinase-1/Akt Signaling Represents a Major Cyclooxygenase-2-Independent Target for Celecoxib in Prostate Cancer Cells. *Cancer Res*. **2004**, 64, 1444-1451.
36. Xu, H. Gao, H.-K. G. Shu, Celecoxib can induce vascular endothelial growth factor expression and tumor angiogenesis, *Mol. Cancer Therapeut*. **2011**, 10, 138-147.
37. K. M. Kasiotis, E. N. Tzanetou, S. A. Haroutounian, Pyrazoles as potential anti-angiogenesis agents: a contemporary overview. *Front. Chem*. **2014**, 2, 78.
38. Miyamoto, N. Sakai, T. Hirayama, K. Miwa, Y. Oguro, H. Oki, K. Okada, T. Takagi, H. Iwata, Y. Awazu, S. Yamasaki, T. Takeuchi, H. Miki, A. Hori, S. Imamura, Discovery of N-[5-({2-[(cyclopropylcarbonyl)amino]imidazo[1,2-b]pyridazin-6-yl}oxy)-2-methylphenyl]-1,3-dimethyl-1*H*-pyrazole-5-carboxamide (TAK-593), a highly potent VEGFR2 kinase inhibitor. *Bioorg. Med. Chem*. **2013**, 21, 2333-2345.
39. L.L. Yang, G. B.Li, S. Ma et.al. Structure–Activity Relationship Studies of Pyrazolo[3,4-*d*]pyrimidine Derivatives Leading to the Discovery of a Novel Multikinase Inhibitor That Potently Inhibits FLT3 and VEGFR2 and Evaluation of Its Activity against Acute Myeloid Leukemia *in Vitro* and *in Vivo*. *J. Med. Chem*. **2013**, 56, 1641-1655.
40. P.A. Harris, A. Boloor, M. Cheung et.al. Discovery of 5-[[4-[(2,3-Dimethyl-2*H*-indazol-6-yl)methylamino]-2-pyrimidinyl]amino]-2-methyl-benzenesulfonamide (Pazopanib), a Novel and Potent Vascular Endothelial Growth Factor Receptor Inhibitor. *J. Med. Chem*. **2008**, 51, 4632–4640.
41. H. Metwally, M.S. Mohamed, E.A. Ragb, Design, synthesis, anticancer evaluation, molecular docking and cell cycle analysis of 3-methyl-4,7-dihydropyrazolo[1,5-*a*]pyrimidine derivatives as potent histone lysine demethylases (KDM) inhibitors and apoptosis inducers. *Bioorg. Chem*. **2019**, 88, 102929.
42. R. Tripathy, A. Ghose, J. Singh et.al. 1,2,3-Thiadiazole substituted pyrazolones as potent KDR/VEGFR-2 kinase inhibitors. *Bioorg. Med. Chem. Lett*. 2007, 17, 1793-1798.
43. M. Saleh, M. G. El-Gazzar, H. M. Aly, R. A. Othman, Novel Anticancer Fused Pyrazole Derivatives as EGFR and VEGFR-2 Dual TK Inhibitors. *Front. Chem*. **2020**, 7, 917.
44. Hamberg, J. Verweij, S. Sleijfer, (Pre-)clinical pharmacology and activity of pazopanib, a novel multikinase angiogenesis inhibitor. *Oncologist*. **2010**, 15, 539-547.
45. L. Chen, C.J. Li, A Remarkably Efficient Coupling of Acid Chlorides with Alkynes in Water, *Org Lett*. **2004**, 6, 3151-3153,
46. H.L. Liu, H.F. Jiang, M. Zhang, W.J. Yao, Q.H. Zhu, Z. Tang, One-pot three-component synthesis of pyrazoles through a tandem coupling-cyclocondensation sequence. *Tetrahedron Lett*. **2008**, 49, 3805-3809.
47. Y. Oguro, N. Miyamoto, K. Okada, T. Takagi, H. Iwata, Y. Awazu, S. Imamura, Design, synthesis, and evaluation of 5-methyl-4-phenoxy-5*H*-pyrrolo[3,2-*d*]pyrimidine derivatives: Novel VEGFR-2 kinase inhibitors binding to inactive kinase conformation, *Bioorg. Med. chem*. **2010**, 18, 7260-7273.